ELSEVIER

Contents lists available at ScienceDirect

Radiation Physics and Chemistry

journal homepage: www.elsevier.com/locate/radphyschem



Structural and magnetic properties of Mn⁺ implanted silicon crystals studied using X-ray absorption spectroscopy techniques

A. Wolska a,*, M.T. Klepka a, K. Lawniczak-Jablonska a, A. Misiuk b, D. Arvanitis c

ARTICLE INFO

Article history: Received 29 September 2010 Accepted 11 February 2011 Available online 18 February 2011

Keywords:
Si:Mn
Implantation
EXAFS
XMCD
Room temperature ferromagnetism

ABSTRACT

The implantation of Mn ions into two Si substrates with different doping (P or B), resistivity and oxygen content was performed at low and high substrate temperatures. Different post-implantation processing was carried out to study its influence on the structural and magnetic properties of these samples. The local order around the Mn atoms was characterized by X-ray absorption fine structure techniques and the magnetic properties of the Mn ionic cores were determined by means of X-ray magnetic circular dichroism measurements. The results are discussed in relation to the structural and macroscopic magnetic properties. It is shown that the amorphous matrix speeds up the formation of $MnSi_x$ inclusions. However, the existence of inclusions or the type of electrically active dopants is not directly related to the magnetic properties. Therefore, in the performed studies, the importance of structural defects on the magnetic properties was confirmed. A localized magnetic moment carried by the Mn ionic cores could not be detected by means of dichroic measurements.

© 2011 Elsevier Ltd. All rights reserved.

1. Introduction

For decades diluted magnetic semiconductors (DMS) have been extensively investigated in the pursuit of novel ferromagnetic materials, which can be used in spintronic devices. Usually, the Mn-doped III-V and II-VI compounds forming DMS have been the center of attention. However, the Si-based DMS have also raised considerable interest, especially after the report that the Mn-implanted Si crystals can be ferromagnetic with a Curie temperature (T_c) higher than 400 K (Bolduc et al., 2005). Main advantage of this material would be the easiness to integrate with the existing technologies and relatively well established procedure to carry out processing at the industrial production. Moreover, the implantation of Mn⁺ ions into a silicon matrix would be a good way of exceeding the solubility limit of Mn in Si. On the other hand, the ferromagnetic properties were also reported for silicon samples implanted with non-magnetic ions, e.g. Si or Ar (Dubroca et al., 2006). Therefore, it is important to understand the origin of magnetic properties in this kind of materials. Some authors (Zhou et al., 2007; Yabuuchi et al., 2008) linked the presence of ferromagnetism with the formation of the Mn₄Si₇ nanoinclusions while the others (Misiuk et al., 2006; Osinniy et al., 2008) have not seen this kind of dependence.

A direct way to check whether the magnetism is related to the Mn atom cores is to perform core level X-ray magnetic circular dichroism (XMCD) studies, which allow to detect the local magnetic moments of the specific element what is not possible in the superconducting quantum interference device (SQUID) measurements. Moreover, establishing a correlation between the magnetic properties and the local atomic structure around Mn atoms could also give important indications on the atomic origins of the magnetic properties. In determining the local atomic structure, the X-ray absorption near edge structure (XANES) and extended X-ray absorption fine structure (EXAFS) techniques are extremely useful. Their main advantage is the element selectivity, which allows to extract information on the atomic surrounding of the Mn atoms even at very low concentrations of this element.

2. Experimental

The samples were prepared by Mn⁺ implantation into (0 0 1) oriented silicon wafers grown by Czochralski (Cz-Si) or by floating zone (Fz-Si) methods. These two silicon single crystals differ in the content of interstitial oxygen atoms. The oxygen concentration was equal to 9×10^{17} cm⁻³ for Cz-Si and 1.6×10^{17} cm⁻³ for Fz-Si. The Cz-Si was doped by B for p-type conductivity and exhibits the resistivity of 12Ω cm. The Fz-Si was doped by P for n-type conductivity and has high resistivity exceeding 100Ω cm.

^a Institute of Physics PAS, al. Lotnikow 32/46, PL-02-668 Warsaw, Poland

b Institute of Electron Technology, al. Lotnikow 46, PL-02-668 Warsaw, Poland

^c Physics Department, Uppsala University, Box 530, 75121 Uppsala, Sweden

^{*} Corresponding author. Tel.: +48 22 843 6601x3348; fax: +48 22 843 6034. E-mail address: wolska@ifpan.edu.pl (A. Wolska).

The implantation energy of the Mn $^+$ ions was of 160 keV and a dose of $1\times10^{16}\,\mathrm{cm}^{-2}$. The projected range of the Mn $^+$ ions was equal to 140 ± 50 nm. The temperature of the Si substrate during implantation was kept at 70 °C in the case of Cz-Si:Mn and at 340 °C for the Fz-Si:Mn samples. The implanted samples were subsequently annealed at temperatures from 275 to 1000 °C under Ar hydrostatic pressure of either 1 bar or 11 kbar for 1–10 h.

To facilitate this discussion the results for the Cz1-Si samples are also presented. They were prepared in the same manner as the Cz-Si samples. The only difference was that the substrate temperature during the implantation was equal to 340 $^{\circ}\text{C}$, the same as for the Fz-Si case.

The EXAFS measurements at the Mn K-edge were carried out at Hasylab (A1 and E4 stations) using a seven element silicon fluorescence detector. The samples were cooled to liquid nitrogen temperature (LN₂) in order to minimize the thermal part of the disorder. The XMCD spectra at the Mn L_{3,2} edges were measured at MAX-lab (beamline I-1011). The measurements were carried out at room temperature (RT) and also checked at LN₂ temperature under an applied magnetic field of 0.1 T, along the X-ray path. The total electron yield (TEY) detection mode was used. Two angles of X-ray incidence were chosen: grazing (20° to the sample surface) and normal (90° to the surface).

3. Results and discussion

Manganese silicides crystallize in many structures with various Mn to Si ratios from 3:1 to 1:1.75. In the case of Mn implantation, it is not likely that the formation of inclusions with high Mn content occurs. In order to confirm this assumption, the XANES spectra were analyzed using theoretical calculations. The *ab-initio* calculations were performed using the FEFF 8.4 (Ankudinov et al., 1998). Several phases such as Mn₃Si, Mn₅Si₂ and Mn₅Si₃, as well as the phases with higher Si content, were considered. The results of the calculations for two phases: one with a high Mn content—Mn₅Si₂ and the other with a low Mn content—Mn₁₅Si₂₆ are presented in Fig. 1 as an example. In the Mn₅Si₂ structure, the Mn atoms are located in seven nonequivalent crystallographic positions (Shoemaker and Shoemaker, 1976) while for Mn₁₅Si₂₆ the Mn atoms occupy eight such positions (Knott et al., 1967). The FEFF calculations were performed for all the clusters created around

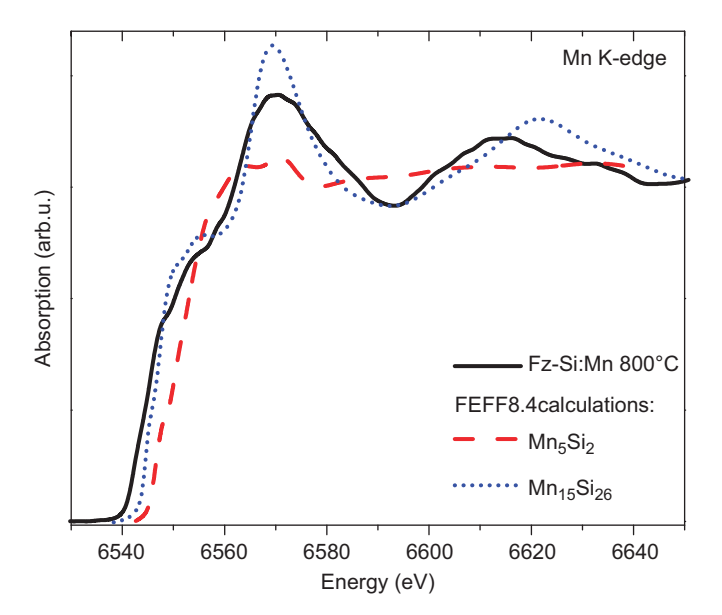


Fig. 1. XANES spectra calculated for Mn_5Si_2 and $Mn_{15}Si_{26}$ compared with the measured one.

each Mn atom in a nonequivalent position and then averaged with the appropriate weight. In Fig. 1 the results of the XANES calculations are compared with an experimental spectrum for one of the samples. The Fz-Si:Mn sample annealed at 800 °C was chosen; however, all the Si:Mn spectra look similar with very broad peaks and lack of sharp features, which indicates the structure with quite high disorder around the absorbing atoms.

As it was expected, the calculated XANES spectrum of the Mn_5Si_2 phase differs significantly from the measured one, while the calculations for the Mn_1Si_{26} phase show similarities (Fig. 1). The Mn_1Si_{26} phase belongs to the family of the so called higher manganese silicides (HMS), together with the Mn_1Si_{19} , Mn_2TSi_{47} and Mn_4Si_7 phases. Their Si/Mn ratio is between 1.70 and 1.75. Their lattice constant a is close to 5.5 Å while c changes from 17 to 118 Å. A detailed comparison of the lattice parameters can be found in the papers by Zhou et al. (2007) or Migas et al. (2008). Miyazaki et al. (2008) revealed that differences in the HMS composition affect mainly the x and y positions of the Si atoms while it almost does not disturb the Mn sites.

As it was mentioned before, the Mn and Si atoms are located in many nonequivalent crystallographic positions. Twelve such positions were found for Mn in the $Mn_{11}Si_{19}$ phase (Schwomma et al., 1964), eight for Mn in the $Mn_{15}Si_{26}$ phase (Knott et al., 1967; Flieher et al., 1967), twenty eight for Mn in the $Mn_{27}Si_{47}$ phase (Zwilling and Nowotny, 1972) and five for Mn in the $Mn_{4}Si_{7}$ phase (Gottlieb et al., 2003). EXAFS, similarly like XANES, provides the average information from all the Mn atoms; therefore, all of them have to be considered in the analysis.

The Artemis and Athena programs (Ravel and Newville, 2005), using the IFEFFIT data analysis package, were applied in the analysis of the EXAFS data. First, the theoretical simulations of the FT spectra for the Mn₁₁Si₁₉, Mn₁₅Si₂₆, Mn₂₇Si₄₇, Mn₄Si₇ phases were performed. Fig. 2 presents simulated spectra that consist of weighted sums of the single scatterings on the Si and Mn atoms located at the distance of up to 3 Å around each Mn central atom. In order to show the distribution of the Si and Mn atoms, the scattering paths on all Si near neighbor atoms and next Mn neighbor atoms were summed separately and also included in Fig. 2. As can be seen, the magnitudes of averaged spheres around Mn atoms look similar. The first peak consists mainly of the Si atoms (8.1-8.26 depending on the phase at average distance $\sim 2.45 \text{ Å}$) while four Mn atoms ($\sim 2.97 \text{ Å}$) dominate in the second one. The average atom distribution around the Mn atoms looks very similar for the HMS phases; therefore, it is not possible to distinguish between them by means of EXAFS.

The analysis of the EXAFS spectrum for each investigated Si:Mn sample was carried out in the same way in order to enable the proper comparison between them. We do not observe the influence of multiple atomic excitations on the background; therefore, a linear background was removed from all spectra. During the fitting the simplest model containing one Si path for the first shell and one Mn path for the second one was used. The passive electron reduction factor was fixed to a value equal to 0.75 estimated by the method described in Ravel (2000) using data of the Cz-Si:Mn sample annealed at 275 °C. This factor is strongly correlated with the coordination number (*N*); therefore, this assumption made possible to find the relative changes in *N* for the investigated samples in order to monitor the effect of the processing.

Figs. 3 and 4 present the evolution of the magnitude of the Fourier Transformed EXAFS oscillations of the Fz-Si:Mn samples (implanted at 340 °C) and Cz-Si:Mn samples (implanted at 70 °C) subsequently processed within the range of 275–1000 °C (under 1 bar or 11 kbar). One can notice that the local crystallographic environment of the Mn atoms mainly depends on the substrate temperature during the implantation and the annealing temperature, the enhanced pressure seems to be of lesser importance

Download English Version:

https://daneshyari.com/en/article/1891643

Download Persian Version:

https://daneshyari.com/article/1891643

Daneshyari.com